







## Development of the nano-composite cement: Application in regulating grouting in complex ground conditions


**WANG Sheng\***  <http://orcid.org/0000-0003-4310-1891>;  e-mail: yongyuandewangsheng@sina.com

**WANG Jing-fei**  <http://orcid.org/0000-0002-8552-4385>; e-mail: 814530304@qq.com

**YUAN Chao-peng**  <http://orcid.org/0000-0003-4775-1138>; e-mail: muyangren@sina.cn

**CHEN Li-yi**  <http://orcid.org/0000-0002-7920-0325>; e-mail: cly@cdut.edu.cn

**XU Shi-tong**  <http://orcid.org/0000-0001-6829-0110>; e-mail: 1085706237@qq.com

**GUO Kai-bin**  <http://orcid.org/0000-0002-2981-6922>; e-mail: 812109142@qq.com

*State Key Laboratory of Geohazard Prevention & Geoenvironment Protection, Chengdu University of Technology, Chengdu 610059, China*

**Citation:** Wang S, Wang JF, Yuan CP, et al. (2018) Development of the nano-composite cement: Application in regulating grouting in complex ground conditions. *Journal of Mountain Science* 15(7). <https://doi.org/10.1007/s11629-017-4729-9>

© Science Press, Institute of Mountain Hazards and Environment, CAS and Springer-Verlag GmbH Germany, part of Springer Nature 2018

**Abstract:** Improvement of the fluidity and setting time of grouting materials has been recognized as an effective approach of seepage prevention in foundation works, and it is quite common to be used for handling severe leakages in complex ground conditions, such as loose, broken and fully fissured stratum. For the purpose of better meeting the engineering requirements, experimental studies were conducted in this study with focus on the nano-composite grouting materials and the related controlled grouting technology. As compared with the commonly used silicate-sulpho-aluminate composite cement, which is characterized by relatively poor rheological property, quick setting time and low strength, the most suitable nano-material with proper reactants were selected intentionally to improve the mentioned attributes of composite cement. Due to the setting time and strength of the targeted cement slurry behaving with poor performance of harmonization to engineering construction problems, hydration synergistic effect of these composites were investigated in our experiments. Results showed that the properties of grouting materials, including initial fluidity, setting time, ideal right-angle thickening, and

early strength and late strength were sufficient to produce an expected grouting application. It is therefore advocated that the refined grouting material could provide a better solution to fix grouting problems in complex ground cementing operations.

**Keywords:** Nano-silica; Silicate-sulpho-aluminate composite cement grout; Controlled grouting; Complex ground conditions

### Introduction

In order to control seepage and underwater erosion in complex crushed strata with steeply sloping joints, a high performance grouting material is generally required. The required grouting material should have a good initial fluidity for adjustable pumping period, short initial setting time, high early strength of the slurry and further a sufficient growth in strength at a later stage. Because the setting time of the common Portland cement is relatively long and its early strength is low, the hardening slurry or cement usually shrinks and therefore in the anti-erosion performance it behaves poorly, which affects its durability (Denise

**Received:** 19 October 2017  
**1<sup>st</sup> Revision:** 28 December 2017  
**2<sup>nd</sup> Revision:** 01 March 2018  
**Accepted:** 08 April 2018

and Paulo 2006). Sulpho-aluminate cement is a new type of cement mainly composed of anhydrous calcium sulphoaluminate and dicalcium silicate as the main mineral. It is desirable for strength increase, seepage prevention and engineering under frost conditions because of its fast hardening, early strength, low shrinkage, good frost resistance and impermeability. However, under some kinds of complex geo-environment, if only using sulpho-aluminate cement without additional agents to be put into grouting, its key performance indexes such as rheology, setting time and slurry strength would be unable to meet the requirements of field engineering applications.

Mixing with different kinds of addition agents can largely regulate the grouting performance of a cement (Janotka and Krajčí 1999; Yu et al. 2016; Shi et al. 2016; Kalashnikov et al. 2016). Researches and experimental applications on the properties of composite cements with certain admixtures had been carried out (e.g., Yan et al. 2016; He et al. 2016; Teixeira et al. 2016; González-Fonteboa et al. 2017; Khomich et al. 2016), and assessment of the performance of such composites ensued. Researches on composite cement had confirmed that the combination of Portland (silicate-) cement with sulpho-aluminate compound, not only kept the original merits of Portland (silicate-) cement, but also exhibited an unexpected "hydration synergistic effect" (different types of cements affected each other in hydration processes and improved hydration reactions, accelerating the hydration and hardening process) (Liu et al. 2016; Saafia et al. 2015). The main improvement included rapid slurry coagulation, shorter final setting time, and right-angle thickening (The thickening curve has the form of a right angle). Due to the synergetic effect of hydration of the compound silicate-sulphoaluminate cement, the improvement of rheology, setting time and consistency of slurry strength can be achieved. It is expected that it can solve the technical problems of grouting in complex situations.

Nano-materials have special structural, physical and chemical properties. They are research concerns in the field of material science, regarded as "the most promising materials in the 21st century" (Al-Saud et al. 2011; Salomaa et al. 2015; Ahmeda et al. 2017). When nano-silica

solution ( $\text{SiO}_2$ ) is added to silicate-sulphoaluminate compound, it can fill voids, to promote cement hydration, to improve the micro-structure of cement-stone contact, and thus it will improve slurry strength, impermeability and anti-erosion capacity.

Comprehensive researches on the suitability of composite grouting materials have not yet widely performed. The pioneered research found that nano-silica solution ( $\text{SiO}_2$ ) with superplasticizer (JSS), early-strength admixture (LC) and mixed with silicate-sulphoaluminate cement, forming a nanocomposite cement-based grouting material, produced a suitable grout satisfying complex grouting procedures. This grouting materials work with controllable rheological property; therefore some grouting procedures are optimized, applicable to engineering purposes (Shen et al. 2013a,b, 2017). It is feasible to increase the rheological property of cement slurry during the construction of a stratum with larger penetrant radius using the construction method of single liquid pump. It is possible to reduce the setting time of a cement slurry when the cement slurry is required to be rapidly solidified in a stratum, and the construction method of double liquid pump can be used. In this study the aim is to examine the performance of such composite mixtures in grouting works.

## 1 Materials and Methods

### 1.1 Experimental materials

The materials used in the experiments were ordinary Portland cement (P.O42.5), which was mainly composed of tricalcium silicate, dicalcium silicate, tricalcium aluminate and tetracalcium aluminate. Sulpho-aluminate cement (R.SAC42.5) mainly composed of anhydrous calcium sulphoaluminate and dicalcium silicate. Nano-silica sol ( $\text{SiO}_2$ ), which is VK-So1B, a transparent liquid with a silica content of  $30\% \pm 2\%$ , which was supplied by Hangzhou Wan Jing New Material Co. Ltd. (Hangzhou, China). The liquid superplasticizer (JSS) and the solid early-strength admixture (LC) were independently developed by the State Key Laboratory of Geohazard Prevention & Geoenvironment Protection of Chengdu University

**Table 1** Used test instruments

Instrument	Model	Manufacturer
Truncated cone with glass plate electronic balance	JY601	Chengdu Dianrui Experimental Instrument Co., Ltd. (Chengdu, China) Shanghai Laidan Industrial Co., Ltd. (Shanghai, China)
Vicat instrument	ISO	Hebei Province Hong Yu Instrument Equipment Co., Ltd. (Hebei, China)
Reducer electric mixer	DD	Hangzhou Instrument Motor Co., Ltd. (Hangzhou, China)
Cement curing box	SBY-40B	Shaoxing Baojia Instrument Co., Ltd. (Shaoxing, China)
Computer hydraulic pressure testing machine	YAW-300	Ji'nan Kai Rui Machinery Equipment Co., Ltd. (Ji'nan, China)
Six-speed rotary viscometer	ZNN-D6B	Qingdao Jiaonan Tongchun Petroleum Machinery Co., Ltd. (Qingdao, China)
Scanning electron microscope	JSM-7500F	Japan Electronics Co., Ltd.
X - ray diffractometer	DX-2700	Dandong Fangyuan Instrument Co., Ltd. (Dandong, China)

of Technology. The main ingredients of superplasticizer JSS was Maleic anhydride, Polyethylene glycol 200 diacrylate and Sodium allylsulfonate.

### 1.2 Experimental equipment

Information about the test instruments and their manufacturers is shown in Table 1.

### 1.3 Experimental method

#### 1.3.1 Measurement of fluidity and pumping capability

Cement slurry fluidity and pumping period were measured in accordance with Chinese Code GB/T8076-2008.

Cement slurry was stirred up for 1 to 2 minutes and quickly poured into the center of a truncated cone with a circular flat glass plate and a scraper attached. The truncated cone was raised up above

the glass plate while starting a stopwatch. After 30s, the maximum diameter of the cement slurry was measured in two perpendicular directions with a ruler (Figure 1). The average value was taken as the fluidity of the cement slurry. Then the time was recorded at the moment that the cement slurry reached a diameter of 14 cm (5.5 in.). This is considered as the time that the slurry can be pumped around.

#### 1.3.2 Measurement of the setting time

Setting time (initial setting time, final setting time) was measured according to Chinese Code GB/T1346 2011.

The cement slurry was poured into a truncated cone, placed under the vicat instrument. The vicat instrument was adjusted according to the operating manual. The test needle was located on the cement slurry surface and then dropped freely at various time intervals into the cement slurry. If the test needle can't penetrate the slurry deeper than a distance from the bottom of 4 mm (0.16 in.), the cement would be considered to be the initial setting state, and the initial coagulation time was recorded at the moment. A ring was attached on the test needle and the needle was dropped again vertically into the cement slurry from the cement surface at different time intervals. As the ring didn't leave the marks on the cement, it is considered as the final setting state of the cement.

#### 1.3.3 Measurement of the rheological parameters

Rheological parameters of cement slurry were determined by SY/ T 5480-1992.

The cement slurry was poured into the six-speed rotary viscometer. The test was performed with different speeds from high to low at regular

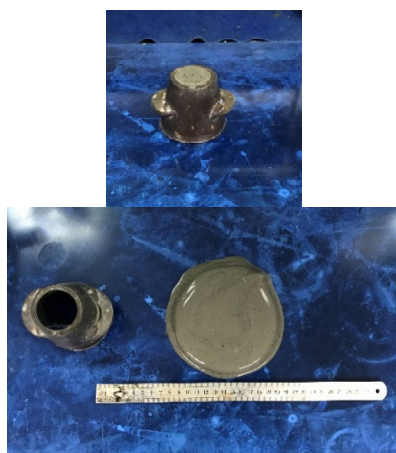


**Figure 1** Measurement of fluidity and pumping capability of the nano-composite cement.

intervals, and the instrument reading values were marked as soon as the pointer measuring shear stress remained stable. These measurements had been executed continuously until the cement slurry lost its fluidity. Experimental results were fitted by MatlabIn 8.0 software, and the Sum of Square Errors (SSE) and the goodness-of-fit ( $R^2$ ) were checked by fitting with four different rheological models delivering the corresponding rheological model parameters for the composite cement.

**1.3.4 Measurement of the compressive strength**

The compressive strength of the cement sample was determined according to Chinese Code GB17671-1999.

The cement slurry was poured into a 70.7 mm × 70.7 mm × 70.7 mm (2.8 in. × 2.8 in. × 2.8 in.) cubic steel mould and kept in a curing box for 3 days. Then the cement sample was placed on a clean and smooth adjustable pressure platform according to the operating manual, and the unconfined compressive test was carried out. The unconfined compressive strengths of the cement samples were recorded at failure and the average value of the compressive strengths of 5 cement samples was obtained by repeated tests.

**1.3.5 Microscopic analysis of the nano-composite cement**

(1) X-ray diffraction

X-ray diffraction (XRD) analysis is one of the most effective methods for phase identification in the material science, which has been widely used to identify the composition of cement hydration products. The cement slurry was poured into a test mould, and placed in a curing box for specific curing times. At the appropriate time the samples were prepared according to the test requirements of XRD, and subjected to X-ray diffraction tests.

(2) Scanning electron microscope

Electron microscopy is a powerful tool to

observe directly the hydration process of a cement. The cement samples were prepared according to the formulas of base mixtures and composite mixtures. After the samples were dried up, the samples were fixed on a metal table with double-sided conductive adhesive. The JSM-7500F scanning electron microscope was used to screen the morphology of the cement samples from different positions with varied magnifications.

**2 Results and Discussions**

**2.1 Properties of the silicate – sulpho-aluminate cement**

In the series of tests, the percentages of Portland cement (P.O 42.5) in all composite cements were increased from 10% to 90%, and accordingly the sulpho-aluminate cement (R.SAC 42.5) dropped from 90% to 10% (Table 2). The water-cement ratio (W/C) was kept 0.45. Table 2 show that the initial fluidity, pumping period, setting time and other test results. The compressive strength values of 9 different composite cement pastes are illustrated in Figure 2.

In Table 2 it can find that with the addition of the proportion of Portland cement (from 10% to 90%), the initial fluidity reveals first a small

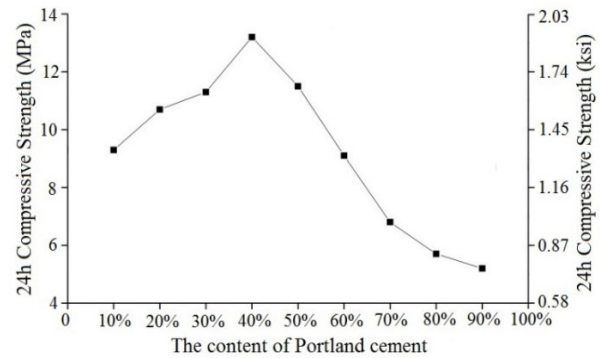


**Figure 2** 24h compressive strength of silicate - sulphoaluminate composite cement slurry.

**Table 2** Properties of silicate – sulpho-aluminate composite cement

P.O 42.5 + R.SAC 42.5	W/C=0.45									
P.O 42.5 (%)	10	20	30	40	50	60	70	80	90	
R.SA C 42.5 (%)	90	80	70	60	50	40	30	20	10	
Initial fluidity (cm (in.))	18 (7.1)	15 (5.9)	19 (7.48)	20 (7.87)	21 (8.27)	22 (8.66)	23 (9.1)	21.5 (8.46)	24 (9.45)	
Pumping period (min)	4	3	3	6	6	7	7	8	28	
Initial setting (min)	17	10	8	11	13	14	18	30	62	
Final setting (min)	25	16	13	16	15	17	21	32	73	

**Notes:** P.O 42.5: Portland cement; R.SA C 42.5: Sulpho-aluminate cement; W/C: Water-cement ratio.



decreasing and then reverses to a small rising trend. The same pattern exists for the “pumpable” period while it is the maximum for 28 minutes at a proportion of Portland cement at 90%. Similarly, the initial setting time and the final setting time also exhibit a tendency to decrease at first and increase later. Intervals between initial setting and final setting are generally short, mostly at values between 2 min and 5 min. As the sulpho-aluminate cements become principal component with the gradual decrease in the proportion of Portland cement, the composite cement hydrates to produce more ettringite, leading the compressive strengths of composite cements to increase first and then decrease with a maximum of about 13 MPa (1.89 KSI) at a proportion of Portland cement to sulpho-aluminate cement ratio 4:6, (Figure 2). As noticed in Table 2, the composite cement characterizes itself as best for grouting reinforcement. For instance, the short interval between the initial and final setting time be advantages for the grouting works as well. This is because the current grouting works have been heavily restricted by the short pumpable period and lower compressive strength of ordinary Portland grout. It is the purpose of this study to develop refined mixture, with a combination of preferable properties (long pumping period, short setting time, good rheology and high strength), which is inclined to a broad applications in engineering practices.

## 2.2 Refinement of mixtures and performance

In order to find a proper mixture ratio, nano-materials were added to a fundamental mixture of 40% P.O42.5 with 60% R.SAC42.5. The influence of the nanometer materials (nano-silica, nanometer calcium carbonate, nano-clay) on grouting properties was tested and analyzed. The main functions of nano-silica in composite cement are as follows:

### (1) Nanometer filling effect

There are abundant micro-pores developing in cement stone during the process of cement hydration. Because cement particles have larger diameter than the sizes of the pores, interspaces between cement stones cannot be filled entirely to such an extent that all pores are completely packed, resulting in low strength of cement stone. The

particle sizes of nano-silica used in the test were 1~100 nm, which would be effectively filled into the pores, reinforcing the strength of the cement stone.

### (2) Crystal nucleus effect

The strong bond between the particles of nano-silica plays a catalytic role, which can eliminate the formation process of the C-S-H nucleation during hydration process. The hydrated calcium silicate gel is transformed from a loose state into a network structure with nano-silica particles as the cores, thus forming a whole dense structure.

It found that nano-silica powder used in the experiments was hardly dissolved in water, therefore no change occurred to the properties of composite cement. After several tests, nano-silica solution was tried to use which was made by an ultrasonic shock mixing process. Nano-silica sol revealed terrific dissolvability and brought out the expected improvement on the grouting performance of the cement. The early-strength admixture (LC) promoted the hydration reaction of cement and produced a large amount of Aft, which united particles into a net structure, making the slurry solidified rapidly and became more dense. Nano-silica with small diameter and large specific surface area can be evenly dispersed in cement, fully filling the micro pores between Aft to make slurry become denser, and it significantly improve the strength of cement stone. Therefore, the early strength of nano-composite cement is higher. The fluidity of the composite cement slurry is mainly changed by the superplasticizer JSS. The combination of nano-SiO<sub>2</sub>+LC+JSS as admixture was determined by comprehensive evaluation.

We added 0.05% SiO<sub>2</sub>, 0.05% LC and 0.3% JSS separately to a series of base fluids to test the pumping duration and the compressive strength of composite cement with a water cement ratio (W/C) of 0.45. The results showed that the pumping time of the base fluid was 6 min if without the addition of admixtures. When 0.05% SiO<sub>2</sub>, 0.05% LC was added to a base fluids, there was little effect (the pumping time remained as 6 to 7 min, and it suggested that the main function of nano-SiO<sub>2</sub> and LC is to promote the compressive strength of composite cement). After adding the self-developed superplasticizer JSS, the pumping time was extended to 22 min.

The effects of admixtures on the compressive

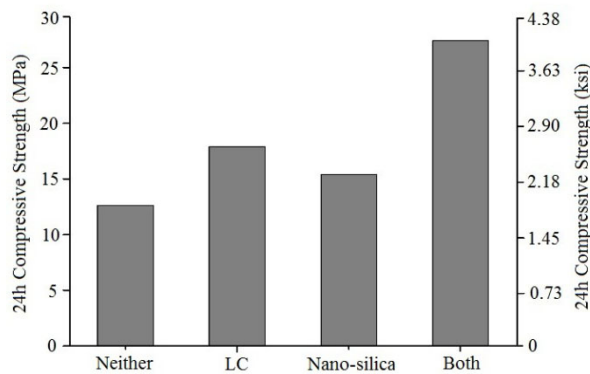


**Figure 3** Effect of the added admixtures to the strength of cement slurry.

strength are shown in Figure 3. After adding the early strength agent LC to the base liquid, the compressive strength of the 24 h slurry increased. The addition of nano-silica alone also increased the strength of the slurry. After adding nano-silica and LC at the same time, the increase in compressive strength is very clear.

### 2.3 Development of nano-composite cement based grouting material

Arising from previous tests, three percentage levels (0.01%, 0.05%, and 0.10% cement mass percentage) of nano-silica and LC were organized to make 9 different combinations for the final experiments. Further, W/C ratio of 0.45 was selected, because it can produce the optimum combination with the maximum 24h compressive strength. The results are shown in Table 3.

In Table 3 it can be seen that the compressive strengths of composite cements increased greatly when both nano-SiO<sub>2</sub> and LC were added into the base fluids, as shown in Figure 3. The compressive strength of sample 8 appeared to be the highest (27.3 MPa) (3.96 KSI).

Further, this optimal combination of nano-SiO<sub>2</sub> and LC were studied for examination of the performance index of the cement if adjusting the water-cement ratio as well as JSS quantity to meet the optimal requirements for engineering constructions. These test results are shown in Table 4.

Kept at a constant W/C, the pumping time of the composite slurry increased with the increases in JSS. If keep JSS content unchanged, the effective pumping period increased with the increment of the water cement ratio (W/C). Considering

**Table 3** Effect of amount of Nano-SiO<sub>2</sub> + LC components on compressive strength

Sample	Nano-SiO <sub>2</sub> (%)	LC (%)	Compressive strength MPa (ksi)
1	0.01	0.01	22.6 (3.28)
2	0.01	0.05	24.6 (3.57)
3	0.01	0.10	20.7 (3)
4	0.05	0.05	23.9 (3.47)
5	0.05	0.10	20.7 (3)
6	0.05	0.01	26.6 (3.86)
7	0.10	0.10	20.9 (3.03)
8	0.10	0.01	27.3 (3.96)
9	0.10	0.05	25.7 (3.73)

**Notes:** LC, the solid early-strength admixture was independently developed by the State Key Laboratory of Geohazard Prevention & Geoenvironment Protection of Chengdu University of Technology.

**Table 4** Effect of JSS component quantity on pumping capacity of a composite grout

Sample	W/C	JSS (‰)	Pumpable period (min)
1	0.45	3	9
2	0.45	4	11
3	0.45	5	14
4	0.45	6	22
5	0.45	7	25
6	0.5	3	13
7	0.5	4	18
8	0.5	5	21
9	0.5	6	31
10	0.5	7	34
11	0.55	3	18
12	0.55	4	21
13	0.55	5	25
14	0.55	6	34
15	0.55	7	38
16	0.6	3	19
17	0.6	4	24
18	0.6	5	29
19	0.6	6	35
20	0.6	7	42

**Notes:** Sample 3, sample 9, and sample 20 were selected as refined mixtures. W/C, Water-cement ratio; JSS, the liquid superplasticizer was independently developed by the State Key Laboratory of Geohazard Prevention & Geoenvironment Protection of Chengdu University of Technology.

material properties, construction conditions, price and other factors, sample 3, sample 9, and sample 20 were selected for short, medium and long term effective pumping times. These three optimized mixtures with the percentages of all their components and the pumpable time are given in Table 5.

**Table 5** The three optimized mixtures with the percentage of all the components and pumping time

	Refined mixtures	Pumping time (min)
1	base fluid +0.50%JSS+0.10%SiO <sub>2</sub> +0.01%LC (W/C = 0.45)	14
2	base fluid +0.60%JSS+0.10%SiO <sub>2</sub> +0.01%LC (W/C = 0.50)	31
3	base fluid +0.70%JSS+0.10%SiO <sub>2</sub> +0.01%LC (W/C = 0.60)	42

**Notes:** JSS, superplasticizer; W/C, Water-cement ratio; LC, early-strength admixture.

**Table 6** Flow rate and the setting time of the three refined mixtures

Optimized mixtures	W/C	JSS (%)	Initial fluidity (cm, (in.))	Flow failure rate	Pumpable period (min)	Initial setting time (min)	Final setting time (min)
1	0.45	5	23 (9.06)	Fast	14	28	32
2	0.5	6	31 (12.2)	Moderate	31	45	49
3	0.6	7	44 (17.3)	Slow	42	54	59

**Notes:** W/C, Water-cement ratio; JSS, superplasticizer.

## 2.4 Properties of nano-composite cement grouting material

### 2.4.1 Fluidity and Setting time

It can be seen in the Table 6 that for the three optimized mixtures, with the increase of water cement ratio or JSS content, the initial fluidity of the grouting materials increased from 23 cm to 44 cm, and the pumping period extended from 14 min to 42 min, the initial setting time from 28 min to 54 min, and the final setting time from 32 min to 59 min. The optimal pumping time to the initial coagulation time interval was between 12 min and 14 minutes, and the initial and final coagulation time interval was less than 5 min. When stirred the nano-composite cement into water, it altered fluidity little in the first place. However, after a certain time, the fluidity drastically decreased mostly due to the rapid thickening of the slurry. The travelling distance of the three optimized mixtures became less than 14 cm at 14 min, 31 min, and 42 min, so the three cement slurries can be pumped within this time range (Figure 4).

It is obvious that the special properties of nano-composite grouts can be controlled by adjusting the composition of the mixtures for some specific engineering requirements. The typical “Right Angle Thickening” (the thickening curve in Figure 4 has a shape of right angle) characteristic of the nano-composite cement-based grouting material provides a good basis for controlled grouting in complex ground material.

### 2.4.2 Rheological properties

The rheological model of the slurry was

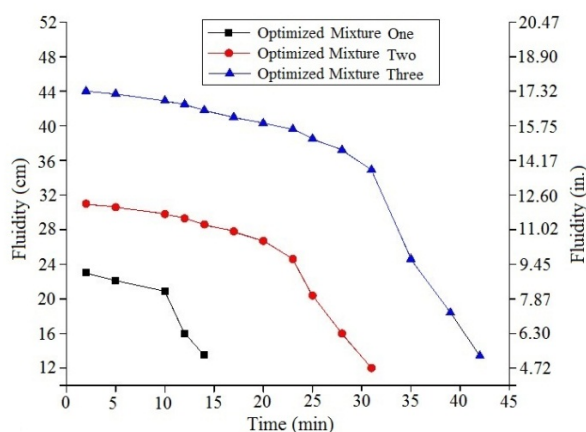


**Figure 4** Fluidity curve of nano-composite cement with the three refined mixtures.

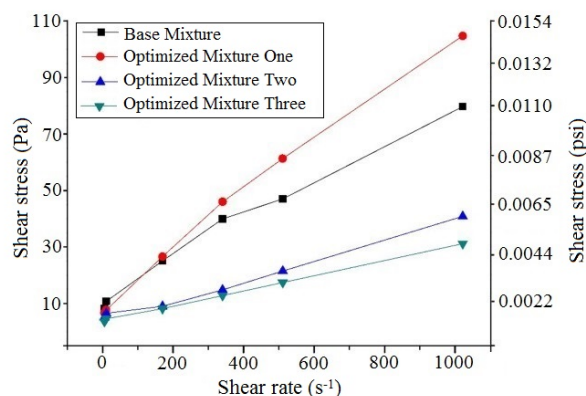


**Figure 5** Shear Stress - Shear Rate of the three refined mixtures.

analyzed by determining its shear stress at different shear rates. The three optimized mixtures were compared with a control mixture of 40% P.O42.5 with 60% R.SAC42.5. The shear stress-shear rate curves obtained are shown in Figure 5.

The degree of the goodness-of-fit ( $R^2$ ) and the Sum of Square Errors (SSE) for grout mixtures were also obtained by fitting the curve using four different rheological models suitable for viscous fluids (Table 7).

Based on the Sum of Square Errors (SSE) and the goodness-of-fit ( $R^2$ ), the Herschel-Bulkley model was confirmed as the most ideal rheological model to characterize the rheological properties of base fluid. And the most suitable rheological model for the mixtures containing JSS and nano-SiO<sub>2</sub> and LC is still the Herschel-Bulkley model.

The rheological properties of the grout are characterized by the apparent viscosity, dynamic shear, flow index and the consistency coefficient in the Herschel-Bulkley model. The mathematical expression of the Herschel Bulkley model is:

$$\tau = \tau_y + K\dot{\gamma}^n \tag{1}$$

where  $\tau$  = Shear stress, Pa;  $\tau_y$  = yield stress, Pa;  $K$  = consistency coefficient;  $\dot{\gamma}$  = Shear rate, s<sup>-1</sup>;  $n$  = flow index.

The yield stress ( $\tau_y$ ) in the Herschel-Bulkley model is the lowest shear stress level at which the fluid begins to flow. The value of the yield stress is mainly related to the type and concentration of the cement in the mixtures. The consistency coefficient ( $K$ ), the viscosity and the shear stress are interrelated. The flow index ( $n$ ) is the non-Newton degree of the fluid within a certain shear rate range. The smaller the flow index is, the stronger is the non-Newtonian degree, giving the cement grout better shear dilution properties. The rheological

properties are shown in Table 8, which shows the following:

(1) Compared to the control mixture, the three optimized mixtures with the same water-cement ratio ( $W/C = 0.5$ ) exhibited decreases in yield stress, consistency coefficient, and apparent viscosity and an increase in flow index. Therefore these mixtures have a better mobility than the control mixture, and obviously a better pumping capacity.

(2) The dynamic shear strength, consistency coefficient and the apparent viscosity of the composite slurry decreased with the increases of water-cement ratio as well as JSS, while the flow index increases. The fast, medium and slow mobility reduction rate of the three mixtures can be explained from their rheological properties.

### 2.4.3 Compressive strength

The compressive strengths of the three refined mixtures of nano-composite cement (Table 5) were tested after 1, 3, 7 and 28 days. The results are shown in Figure 6 and Figure 7.

The 24 hours compressive strengths demonstrate a reduction with the increases of water cement ratio. But all the samples have compressive greater than 18 MPa. Subsequent tests were also performed after 3, 7, and 28 days to explore the change of the compressive strength at the later stages of hydration. These test results are shown in Figure 7.

The strength curves, in Figure 7 depict the same trend with a faster growth in the beginning

**Table 7** Goodness of fit ( $R^2$ ) and the residual value SSE of the composite cement grout with the three refined mixtures

		Base mixtures	Optimized mixture 1	Optimized mixture 2	Optimized mixture 3
Bingham model	$R^2$	0.965	0.991	0.988	0.999
	SSE	102.076	48.996	8.57823	0.459
Power - law model	$R^2$	0.968	0.993	0.923	0.945
	SSE	91.760	41.340	55.917	23.452
Herschel-Bulkley model	$R^2$	0.987	0.999	0.997	0.999
	SSE	37.007	1.992	1.824	0.412
Casson model	$R^2$	0.983	0.999	0.956	0.983
	SSE	37.251	3.756	32.108	7.356

**Table 8** Rheological parameters of the composite cement grout with the three refined mixtures

	Dynamic shear ( $\tau_y$ ) Pa (psi)	Flow index ( $n$ )	Consistency coefficient ( $K$ )	Apparent viscosity ( $\mu_a$ ) MPa·s (KSI·s)
Base mixtures	7.436 (0.0011)	0.734	0.442	78 (11.3)
Refined mixture 1	5.336 (0.0008)	0.834	0.307	69 (10)
Refined mixture 2	4.496 (0.00065)	1.203	0.109	40 (5.8)
Refined mixture 3	3.877 (0.00056)	1.521	0.023	30.5 (4.42)



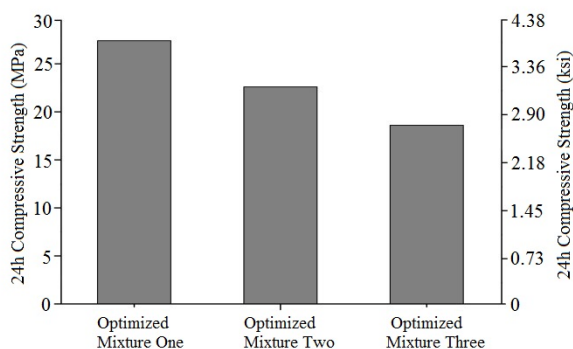


**Figure 6** 24h Compressive strength of the nano-composite cement with the three refined mixtures.

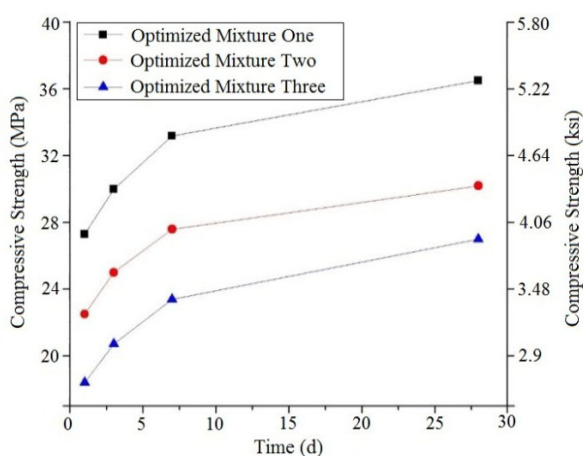


**Figure 7** Compressive strength growth of the nano-composite cement with refined mixtures.

and a slower growth at a later stage. The maximum compressive strength for the three mixtures ranges between 26 MPa and 37 MPa after 28 days, which indicates that the composite cement meets the requirements of pumping duration and setting time, while also the strength development is favorable. JSS had little effect on the improvement of compressive strength of the cement at the same water-cement ratio. Its compressive strength varies within 0.5 MPa, which will not affect the actual engineering applications.

**2.5 Analysis of the microcosmic characteristics of the nano-composite cement mixtures**

**2.5.1 Analysis of X - ray diffraction (XRD) results**

The hydration products of cement samples with different curing times (12h, 24h, 72h) were scanned and analyzed by X-ray diffraction method,

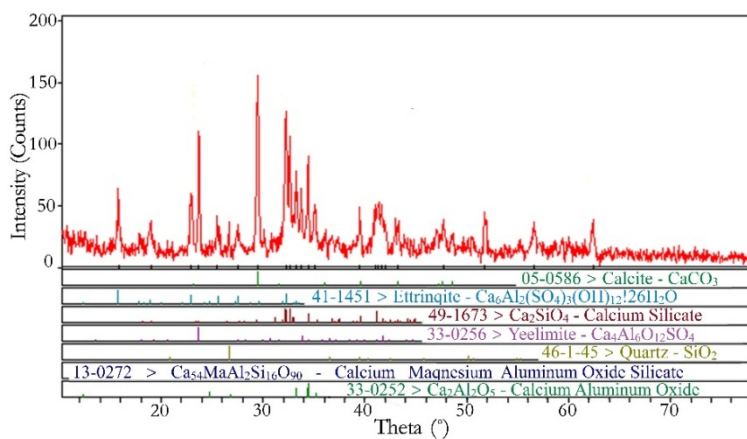
and High Score software was used to visualize XRD photos in Figure 8.

The High Score software analysis confirmed that the hydration reaction of the nano-composite cement created ettringite (AFt), calcium sulfate, calcium hydroxide (CH), aluminium hydroxide gel (AH<sub>3</sub>) and calcium silicate gel (C-S-H). It was observed that after 12h curing time, a large amount of ettringite (AFt), calcium hydroxide, aluminium hydroxide gel (AH<sub>3</sub>) were found in the hydrated product, but just a small amount of calcium silicate gel (C-S-H). After 24h the amount of calcium hydroxide decreased, whereas ettringite (AFt), aluminium hydroxide gel (AH<sub>3</sub>) and calcium silicate gel (C-S-H) increased. Aluminium hydroxide gel (AH<sub>3</sub>) filled the pores of the ettringite (AFt), thereby increasing the compressive strength of the cement. After 72h curing time, the amount of ettringite (AFt) came to stabilize, and calcium silicate gel (C-S-H) content had increased much, which greatly improved the density of the hardened cement structure. As view of the figures reveals that the content of Nano-silica in the hardened cement structure remains basically unchanged, indicating that Nano-silica plays the role of a catalyst in the system, while filling the tiny gaps between the structures to further enhance the compressive strength of nanocomposite hardened cement.

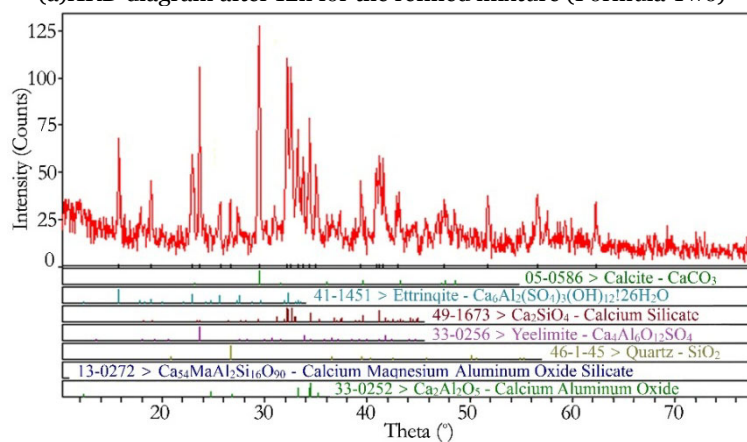
**2.5.2 Analysis by scanning electron microscope**

Scanning electron microscopy (SEM) was used to observe and analyze the micro structure of the cement mixture at different curing times (12h, 24h, and 72h). The samples were observed with magnification factors of 3000 and 5000. The photos of the cements with a base mixture are shown in Figure 9 and with the optimized mixture no 2 (Table 5) of the nano-composite cement are shown in Figure 10.

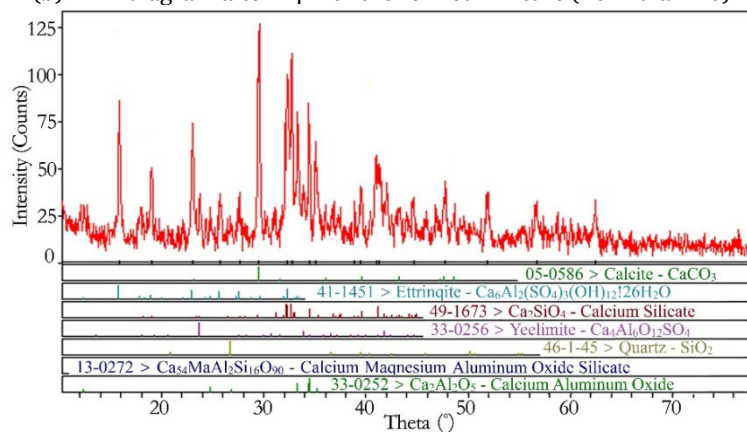
As viewed on the scanned photos in Figure 9, a small amount of needle-like ettringite (AFt), lamellar calcium hydroxide (CH), calcium silicate gel (C-S-H) and aluminium hydroxide gel (AH<sub>3</sub>) can be identified in the basic mixture, which had performed 12h curing treatment with a lower strength than that of the cement containing the optimized mixture 2 (Figure 10). With the increase of curing period to 24h, an amount of ettringite



(a) XRD diagram after 12h for the refined mixture (Formula Two)



(b) XRD diagram after 24h for the refined mixture (Formula Two)



(c) XRD diagram after 72h for the refined mixture (Formula Two)

**Figure 8** XRD diagram at different curing stages for the refined mixture (Formula Two) of the nano-composite cement.

(Aft) needles with variable lengths increased gradually. By 72h, ettringite (Aft) grows to staggered columnar crystals. A small amount of calcium silicate gel (C-S-H) turn into the column-shaped crystals, and some gaps still existed in the structure. This is mainly due to the hydration products containing more ettringite (Aft) and less

gel, while the gel in the hydration products cannot fully fill the gaps between ettringite (Aft), thus restricting the strength growth of the basic mixture cement.

In Figure 10 there exhibit SEM images of the hardened mixture no 2 nano-composite cement. After 12h curing time, a large amount of ettringite (Aft) needles can be identified in the refined hardened cement structure, and lamellar calcium hydroxide (CH), calcium silicate gel (C-S-H) and aluminum hydroxide gel (AH3) are also visible. This interprets why the early strength of the hydrated sample is higher than that of the basic mixture. After 24h the gelatinous coating layers of the hydration products were wrapped up in the agglomeration of the needles of ettringite (Aft) and the lamellar calcium hydroxide (CH). At 72h, the needle-like ettringite (Aft) developed into columnar crystals, and the gaps between the ettringite (Aft) crystals were significantly reduced, thus forming a dense reticular structure, so that hardened cement has high strength.

A comparison of Figure 9 with Figure 10 suggests that:

- 1) The amount of ettringite (Aft) crystals in the refined mixture is higher larger than that in the base mixture, and its diameter is larger.
- 2) The calcium silicate gel (C-S-H) and aluminum hydroxide gel (AH3) in the Nano-composite cement effectively fill the gaps of the structure, making it more compact.

### 3 Conclusions

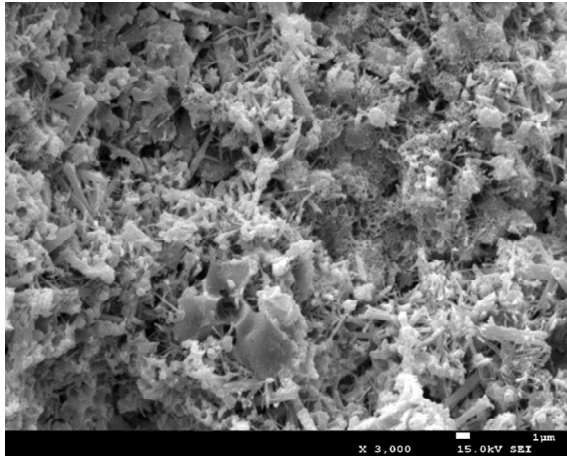
(1) Silicate-sulpho-aluminate composite cement slurry is characterized by the short setting time and low compressive strength. It has been observed, when sulpho-aluminate cement became a predominant component along with gradual decrease in the proportion of Portland cement, the compressive strength of the composite cement first

increased and then decreased, which achieved a maximum at a proportion ratio of Portland cement and sulpho-aluminate cement of the order 4:6.

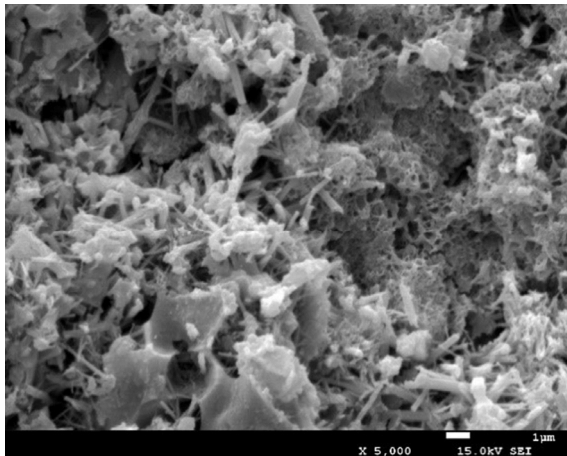
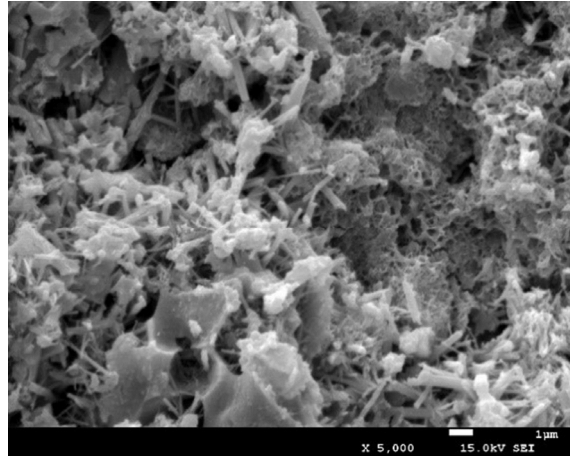
(2) Nano-SiO<sub>2</sub>, superplasticizer (JSS, developed in this study) and early-strength

admixture (LC) can be added to the base fluid to regulate the rheology, setting time and strength of the grout in order to meet the requirements of common engineering practice.

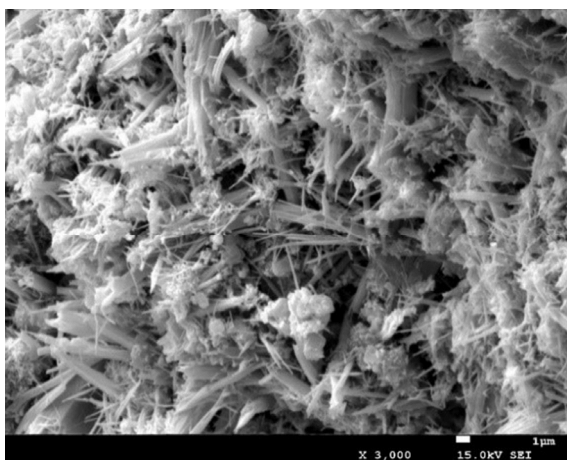
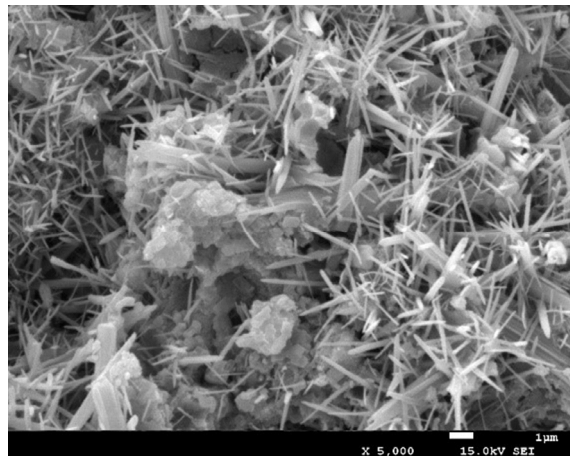
(3) Herschel-Bulkley rheological model can



(a) SEM diagram after 12h curing of the composite cement basic mixture (× 3000, × 5000)



(b) SEM diagram of the 24h curing of the composite cement basic mixture (× 3000, × 5000)



(c) SEM diagram of the 72h curing of the composite cement basic mixture (× 3000, × 5000)

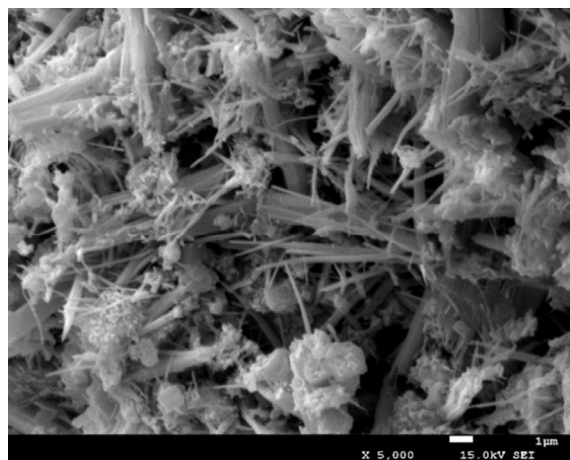


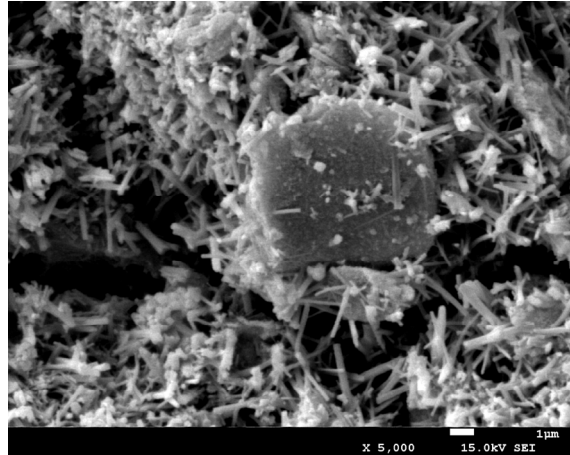
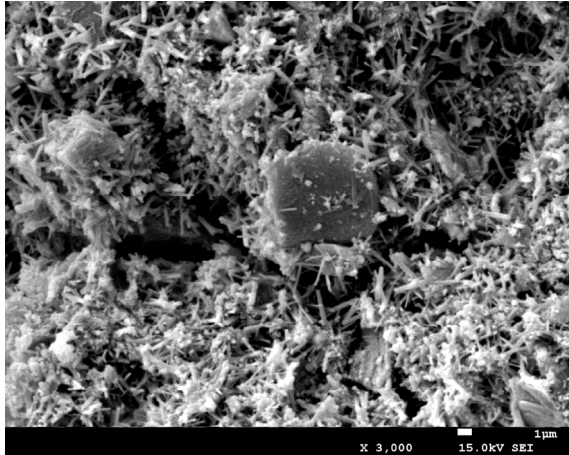
**Figure 9** SEM diagrams of the composite cements with the composite cement basic mixtures.



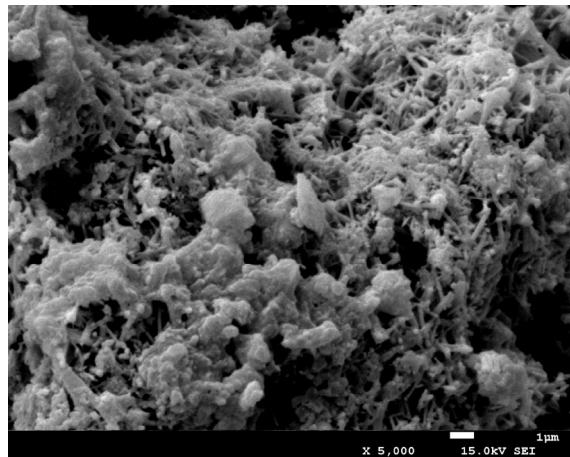
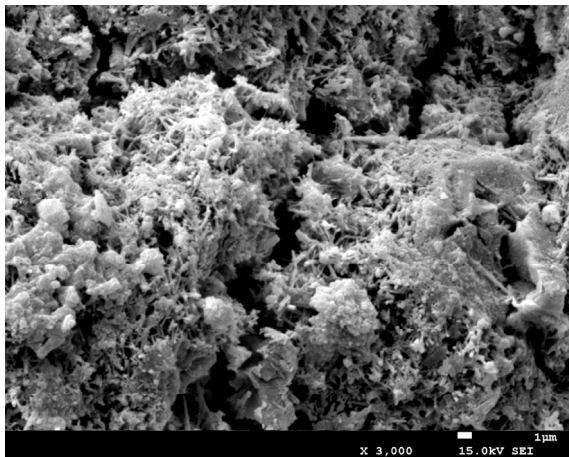
properly describe the rheological properties of the nano-composite cement. The effects of Superplasticizer (JSS) on the rheological properties are due to the properties of the dynamic shear, flow index, consistency coefficient and apparent

viscosity.

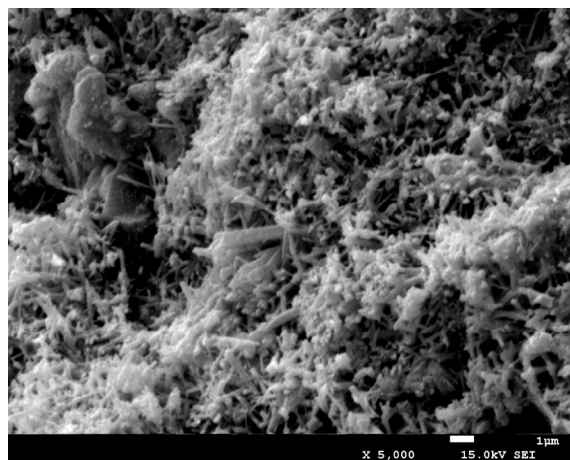
(4) X-ray diffraction (XRD) and scanning electron microscopy (SEM) were used to study the composition and micro morphology of the hydration products in the Nano-composite cement.



(a) SEM diagram after 12h curing of the refined mixture two of the nano-composite cement ( $\times 3000$ ,  $\times 5000$ )



(b) SEM diagram after 24h curing of the refined mixture two of the nano-composite cement ( $\times 3000$ ,  $\times 5000$ )



(c) SEM diagram after 72h curing of the refined mixture two of the nano-composite cement ( $\times 3000$ ,  $\times 5000$ )

**Figure 10** SEM diagrams of the refined mixture two of the nano-composite cement.

In the early stages of hydration, the silicate mineral (C<sub>3</sub>S) reacted with water to produce large amounts of calcium hydroxide (CH), and accelerated the formation of ettringite (AFt), which is the key to the hydration effect of the composite cement grouts. At the same time, calcium silicate gel (C-S-H) and aluminum hydroxide gel (AH<sub>3</sub>) were produced, which filled the pores in the cement structure and maintained the growth of the strength of the composite hardened cement.

The composition of the three refined mixtures with favorable properties for grouting material is simple and easy to produce. These mixtures have exceptional properties, which can be used to complex ground repairing treatment, emergency rescue and

disaster relief projects, as well as drilling and plugging and the renovation of old buildings.

## Acknowledgements

This research was funded by National Natural Science of China (Grant Nos. 41672362), Key Projects of Sichuan Provincial Department of Education (Grant No.16ZA0099) and the State Key Laboratory of Geohazard Prevention & Geoenvironment Protection (Grant No. SKLGP2017Z011). Some of the experiments presented in this paper were conducted at Chengdu University of Technology.

## References

- Silva Denise A, Monteiro Paulo JM (2006) The influence of polymers on the hydration of Portland cement phases analyzed by soft X-ray transmission microscopy. *Cement and Concrete Research* 36(8): 1501-1507.  
<https://doi.org/10.1016/j.cemconres.2006.05.010>
- Janotka I, Krajčí L (1999) An experimental study on the upgrade of sulfoaluminate-belite cement systems by blending with Portland cement. *Advances in Cement Research* 11(1): 35-41.  
<https://doi.org/10.1680/adcr.1999.11.1.35>
- Yu XN, Qian CX, Xue B (2016) Loose sand particles cemented by different bio-phosphate and carbonate composite cement. *Construction and Building Materials* 113: 571-578.  
<https://doi.org/10.1016/j.conbuildmat.2016.03.105>
- Shi ZG, Shi CJ, Zhao R, et al. (2016) Factorial design method for designing ternary composite cements to mitigate ASR expansion. *Journal of Materials in Civil Engineering* 28(9): 1943-5533.  
[https://doi.org/10.1061/\(ASCE\)MT.1943-5533.0001568](https://doi.org/10.1061/(ASCE)MT.1943-5533.0001568)
- Kalashnikov VI, Belyakova EA, Moskvina RN (2016) Selecting the Type of the Control Setting Composite Cement-Ash Binder. *Procedia Engineering* 150:1631-1635.  
<https://doi.org/10.1016/j.proeng.2016.07.143>
- Yan XT, Cui HZ, Qin QH, et al. (2016) Study on utilization of carboxyl group decorated carbon nanotubes and carbonation reaction for improving strengths and microstructures of cement paste. *Nanomaterials* 6(8): 1-12.  
<https://doi.org/10.3390/nano6080153>
- He Y, Zhang X, Gu MD, et al. (2016) Effect of organosilane-modified polycarboxylate-superplasticizer on fluidity and hydration process of cement paste. *Journal of the Chinese Ceramic Society* 44(8): 1166-1172.  
<https://doi.org/10.3390/nano6080153> (In Chinese)
- Teixeira KP, Rocha IP, Carneiro LDS, et al. (2016) The effect of curing temperature on the properties of cement pastes modified with TiO<sub>2</sub> Nanoparticles. *Materials* 9(11): 952.  
<https://doi.org/10.3390/ma9110952>
- González-Fontecha B, Carro-López D, de Brito J, et al. (2017) Comparison of ground bottom ash and limestone as additions in blended cements. *Materials and Structures* 50(1): 84.  
<https://doi.org/10.1617/s11527-016-0954-x>
- Khomich VA, Emralieva SA, Tsyguleva MV (2016) Nanosilica modifiers for cement mortars. *Procedia Engineering* 152: 601-607.  
<https://doi.org/10.1016/j.proeng.2016.07.662>
- Liu JQ, Li JY, Ye JD, et al. (2016) Setting behavior, mechanical property and biocompatibility of anti-washout wollastonite/calcium phosphate composite cement. *Ceramics International* 42(12): 13670-13681.  
<https://doi.org/10.1016/j.ceramint.2016.05.165>
- Mohamed S, Leung T, Jason F, et al. (2015) Enhanced properties of graphene/fly ash geopolymeric composite cement. *Cement and Concrete Research* 67: 292-299.  
<https://doi.org/10.1016/j.cemconres.2014.08.011>
- Al-Saud TSM, Bin Hussain MAA, Batyanovskii EI, et al. (2011) Influence of carbon nanomaterials on the properties of cement and concrete. *Journal of Engineering Physics and Thermophysics* 84(3):546-553.  
<https://doi.org/10.1007/s10891-011-0503-y>
- Nasution A, Imran I, Abdullah M, et al. (2015) Improvement of concrete durability by nanomaterials. *Procedia Engineering* 125: 608-612.  
<https://doi.org/10.1016/j.proeng.2015.11.078>
- Sumair Faisal Ahmeda, Khalida M, Rashmib W, et al. (2017) Recent progress in solar thermal energy storage using nanomaterials. *Renewable and Sustainable Energy Reviews* 67: 450-460.  
<https://doi.org/10.1016/j.rser.2016.09.034>
- Shen SL, Wang ZF, Horpibulsuk S, et al. (2013) Jet-Grouting with a newly developed technology: The Twin-Jet Method. *Engineering Geology* 152(1): 87-95.  
<https://doi.org/10.1016/j.enggeo.2012.10.018>
- Shen SL, Wang ZF, Yang J, et al. (2013). Generalized approach for prediction of jet grout column diameter, *Journal of Geotechnical and Geoenvironmental Engineering* 139(12): 2060-2069.  
[https://doi.org/10.1061/\(ASCE\)GT.1943-5606.0000932](https://doi.org/10.1061/(ASCE)GT.1943-5606.0000932)
- Shen SL, Wang ZF, Cheng WC (2017). Estimation of lateral displacement induced by jet grouting in clayey soils. *Géotechnique* 67(7): 621-630.  
<https://doi.org/10.1680/geot./16-P-159>